

XMM-Newton Observations of the Seyfert 2 Galaxy NGC 7590: the Nature of X-ray Absorption

X. W. Shu¹, T. Liu¹, & J. X. Wang¹

ABSTRACT

We present the analysis of three *XMM-Newton* observations of the Seyfert 2 galaxy NGC 7590. The source was found to have no X-ray absorption in the low spatial resolution *ASCA* data. The *XMM-Newton* observations provide a factor of ~ 10 better spatial resolution than previous *ASCA* data. We find that the X-ray emission of NGC 7590 is dominated by an off-nuclear ultra-luminous X-ray source and an extended emission from the host galaxy. The nuclear X-ray emission is rather weak comparing with the host galaxy. Based on its very low X-ray luminosity as well as the small ratio between the 2-10 keV and the [O III] fluxes, we interpret NGC 7590 as Compton-thick rather than being an "unobscured" Seyfert 2 galaxy. Future higher resolution observations such as *Chandra* are crucial to shed light on the nature of the NGC 7590 nucleus.

Subject headings: galaxies: active — galaxies: individual (NGC 7590) — galaxies: nuclei — X-rays: galaxies

1. Introduction

According to the standard unification model for active galactic nuclei (AGN), Seyfert 2 galaxies are intrinsically the same as Seyfert 1 galaxies. The observed differences between the two types of Seyfert galaxies are primarily due to an orientation effect (Antonucci 1993). The absence of broad emission lines in the optical spectra of Seyfert 2 galaxies is due to obscuration by an optically thick structure (the so-called dusty torus) from our line of sight. Optical spectropolarimetry observations have detected hidden broad emission lines in a large fraction of Seyfert 2 galaxies (Moran et al. 2000; Tran 2001), providing strong evidence in favor of the unification model. Further support for this model is given by the X-ray studies that have demonstrated that many Seyfert 2 galaxies are absorbed by large hydrogen column densities (typically $N_{\text{H}} > 10^{23} \text{ cm}^{-2}$; e.g., Risaliti, Maiolino & Salvati 1999).

¹CAS Key Laboratory for Research in Galaxies and Cosmology, Department of Astronomy, University of Science and Technology of China, Hefei, Anhui 230026, China, xwshu@mail.ustc.edu.cn

However, recent observations have shown that a fraction of type 2 AGNs show no or very low X-ray absorption measured from their X-ray spectra ($N_{\text{H}} < 10^{22} \text{ cm}^{-2}$; e.g., Pappa et al. 2001; Panessa & Bassani 2002; Walter et al. 2005; Gliozzi, Sambruna & Foschini 2007), apparently in contrast to the standard unification model. Panessa & Bassani (2002) estimate the percentage of this type of source in the range 10%–20%. This number is larger than that found by Risaliti et al. (1999) in a sample of Seyfert 2 galaxies (4%), but consistent with the estimate made by Caccianiga et al. (2004, 12%). X-ray unabsorbed Seyfert 2 galaxies may result from the dust reddening intrinsic to the broad line region (BLR) rather than the orientation-based obscuration effects (Barcons, Carrera & Ceballos 2003; Corral et al. 2005). Alternatively, the unabsorbed Seyfert 2 galaxies may genuinely lack the BLR as a result of low accretion rate (Georgantopoulos & Zezas 2003; Bianchi et al. 2008; Panessa et al. 2009). In other words, low-accretion rate systems may not form a stable BLR (see Nicastro 2000 for the model), so they would not show broad lines in their optical spectra, and not necessarily being obscured in X-ray. Though the discovery of "unobscured" type 2 AGNs has important implications for the current unification model (i.e., in addition to the orientation effects, other physical effects should be invoked to interpret the difference observed between type 1 and type 2 AGNs), only few objects have yet been conclusively proven as a class.

It has been argued that some "unobscured" Seyfert 2 galaxies are actually Compton-thick (e.g., Pappa et al. 2001), in which the direct nuclear component below 10 keV is completely suppressed and we would only witness an unabsorbed spectrum due to scattered nuclear radiation and/or host galaxy emission from a circumnuclear starburst. More recently, Brightman & Nandra (2008) presented a detailed spectral analysis of six unabsorbed Seyfert 2 galaxies, and found that four out of them are in fact heavily obscured (see also Ghosh et al. 2007). In addition, Shi et al. (2010) presented a multi-wavelength study of a sample of unobscured Seyfert 2 galaxies, and found that most of them are actually intermediate-type AGNs with broad emission lines or Compton-thick sources. Therefore, one has to be cautious in identifying the candidates of the unabsorbed Seyfert 2 galaxies.

In this paper, we present new *XMM-Newton* observations of NGC 7590, one of the so-called "unobscured" Seyfert 2 galaxies. NGC 7590 ($z = 0.005$) belongs to the extended $12 \mu\text{m}$ sample (Rush, Malkan & Spinoglio 1993). No broad $\text{H}\alpha$ emission line is visible in either direct or polarized light (Heisler, Lumsden & Bailey 1997). The first X-ray spectrum observed by *ASCA* was analyzed by Bassani et al (1999). Their best-fit model is an unabsorbed power law with $\Gamma = 2.29_{-0.13}^{+0.20}$, and $N_{\text{H}} < 9.2 \times 10^{20} \text{ cm}^{-2}$. No Fe K emission line is detected in the *ASCA* data. *ROSAT* HRI imaging has shown that there is an off-nuclear ultra-luminous X-ray source (ULX) that is probably associated with the galaxy NGC 7590 (Colbert & Ptak 2002). The better spatial resolution of *XMM-Newton* allows us to see more directly the X-ray emission from the nuclear region. In the following, a cosmology with $H_0 = 70 \text{ km s}^{-1}$

Mpc⁻¹, $\Lambda = 0.73$, and $\Omega = 1$ is assumed throughout.

2. Observation and Data Reduction

The *XMM-Newton* pointing observation of NGC 7590 (denoted OBS 1) was made on 2007 April 30 for a duration of about 45 ks. Besides the pointing observation, the source was also detected ~ 9 arcmin away from the center of the field of view (FOV) of NGC 7582 *XMM-Newton* observations during revolution 267 (2001 May, OBS 2) for ~ 23 ks and revolution 987 (2005 April, OBS 3) for ~ 102 ks. The calibrated event lists for both the pn and the MOS observations were extracted using the EPCHAIN and EMCHAIN pipeline tasks provided by the *XMM-Newton* Science Analysis System (SAS) version 9.0.0, using the latest calibration files available at the time of analysis (2009 August). In our analysis we deal only with events corresponding to patterns 0-4 for the pn and 0-12 for the MOS instruments. We excluded the epochs of high background events with SAS task *espfilt*. As an instance, we plot in Figure 1 the pn and MOS1 light curves of OBS1 (black), which was heavily polluted by high background flares, together with the derived good time intervals (green) by *espfilt*. The log of all the *XMM-Newton* observations with net exposure times is shown in Table 1. Details of both source and background spectra extraction are shown in Section 3.2.

3. Results

3.1. Imaging and Radial Profiles

In order to improve the signal-to-noise ratio (S/N) and fully utilize the spatial resolution of *XMM-Newton*, we extracted a co-added MOS image from three observations, which has better spatial resolution than pn detector, and re-binned with a pixel size of $1.1''$ (1 MOS pixel). The resultant image is displayed in Figure 2 (a). The cross marks the optical center of the galaxy. A bright point-like source (source X-1) is detected by *XMM-Newton* about $25''$ away from the galaxy nucleus, which was originally detected in the *ROSAT* All-Sky Survey, identified as a ULX by Colbert & Ptak (2002).

It can be seen from Figure 2 (a) that the emission of NGC 7590 is resolved at the *XMM-Newton* spatial resolution, extending to tens of arcsec from the center. To quantify this, we first extract the radial profile of the X-ray emission from NGC 7590. To avoid the contamination from the bright off-nuclear X-1, only photons below the dashed line in Figure 2. (a) were extracted with $1.1''$ annular bins. The radial profile for X-1 was also extracted

(without excluding the extended emission from NGC 7590) for comparison. The resulting radial profiles normalized to the peak brightness of NGC 7590 are shown in Figure 2(c). We then fitted the radial profiles with the MOS point-spread function (PSF) model from calibration files using the SAS routine *eradial*. It is obvious in the figure that the radial profile of NGC 7590 significantly differs from that of the off-nuclear source X-1 and MOS PSF model out to radii of $\sim 30''$, showing that the X-ray emission from NGC 7590 is clearly extended. The radial profile of the ULX is in crude agreement with the PSF model, as expected from a point source emission.

We further used SciSim (Version 2.1) to simulate a MOS image of two point sources at the same position of the ULX and the nucleus of NGC 7590. We first extracted the X-ray counts from the observed image for the ULX within an aperture responding to the $\sim 50\%$ encircled energy radius ($\sim 9''$)¹, and estimated total net counts of ~ 1730 for ULX after aperture correction. We then subtracted 1730 from the total counts of ULX plus NGC 7590 within $40''$ radius circle and obtained net counts of ~ 1380 for NGC 7590 itself. In our simulation, we assumed that both NGC 7590 and ULX would have a power law spectrum with $\Gamma = 1.7$. Local background was added to the simulated image and the result is shown in Figure 2(b). By comparing the simulated image with the observed one, we see that the observed X-ray emission from NGC 7590 is clearly extended.

We also created a co-added pn image (excluding OBS 3)² with a pixel size of $4''$ (1 pn pixel), and extracted radial profiles from it for NGC 7590 and ULX. Figure 2(d) and (f) show the resulting pn image and radial profiles, which are similar to that of MOS, confirming that the X-ray emission from NGC 7590 is extended. We also present archival ROSAT HRI image for NGC 7590 (Figure 2(e)), which has even better spatial resolution than *XMM-Newton*. However, the HRI image is too shallow for more detailed spatial analysis, and its soft X-ray coverage prevents us from estimating the nuclei hard X-ray emission.

There is possibility that the observed spatial extent of NGC 7590 and ULX is due to the alignment errors when adding images of three *XMM-Newton* observations for both pn and MOS data respectively. To test this, we extracted the radial profile of X-ray emission of NGC 7590 and ULX, using only MOS image of OBS 3 (Figures 3.(a) and (d)), which has the longest exposure. Compared to Figures 2.(a) and (c), we do not found significant difference in the spatial extent of NGC 7590 and ULX, indicating it is unlikely that the

¹Which means $\sim 50\%$ of all the X-ray photons are encircled within this radius. See *XMM-Newton* Users Handbook, Section 3.2.1

²There are bad columns across the galaxy nucleus in the pn image of OBS 3. We also excluded this exposure from the following spectral analysis for NGC 7590.

observed extended emission of NGC 7590 is caused by image alignment errors. Figures. 3(b) and (c) show the soft-band (0.5–2 keV) and hard-band (2–10 keV) MOS images of OBS 3, and Figures (e) and (f) are the extracted radial profile, respectively. It can be seen that the spatial extent of soft-band emission of NGC 7590 and ULX agrees well with previous results. All these results suggest that the ULX is a point-like source, but the X-ray emission of NGC 7590 is clearly extended. Indeed, it is presumable that the hard-band image of NGC 7590 will be more point-like. However, as one can see from Figure. 3(c), the hard-band emission of NGC 7590 is relatively rather weak. Due to the poor S/N of the radial profile of NGC 7590 (Figure. 3(f)), we cannot tell whether its hard-band emission is extended or more point-like.

3.2. Spectral Analysis

XMM spectra for NGC 7590 and X-1 were both extracted for spectral analysis. For ULX X-1, to minimize the contamination from the extended emission in NGC 7590, we extracted source spectra using a 9'' radius circle (encircles $\sim 50\%$ of all the X-ray photons at off-axis angles less than 10 arcmin on the MOS detector, see Section 3.1) for both pn and MOS cameras, and aperture correction was applied after spectral fitting. For NGC 7590, we extracted source spectra from a circular region with a radius of 40'' centered at the galaxy nucleus, but excluded all photons above the dashed line in Figure 2(a) to reduce the pollution from X-1. Assuming that the X-ray emission from NGC 7590 is symmetric to the dashed line, hereafter we applied flux correction by a factor of 2 to the spectral fitting results to estimate the total X-ray flux from NGC 7590 (excluding X-1). For both pn and MOS data, the background events were then extracted from a source-free area on the same CCD using two circular regions with a combined area ~ 4 times larger than the source region. The response matrix and ancillary response file for the pn spectrum were generated using the RMFGEN and ARFGEN tools within the SAS software.

We examined the source light curves of NGC 7590 and ULX, and found no significant intra-exposure variations. No spectral variations between individual exposures were detected either through preliminary spectral fitting. Hereafter, we combined spectra from individual exposures to increase the spectral quality and finally obtained one pn and one MOS spectra for each source (NGC 7590 and X-1). The combined spectra were then grouped to have at least 1 count per bin, and the *C*-statistics (Cash 1979) was adopted for minimization. Spectral fitting was performed jointly to the pn and MOS data in the 0.3–8 keV range using XSPEC (version 11.3.2). All statistical errors given hereafter correspond to 90% confidence for one interesting parameter ($\Delta\chi^2 = 2.706$), unless stated otherwise. In all of the model

fitting, the Galactic column density was fixed at $N_{\text{H}} = 1.96 \times 10^{20} \text{ cm}^{-2}$ (Dickey & Lockman 1990). All model parameters will be referred to in the source frame.

NGC 7590: We first performed the spectral fitting with a simple absorbed power law. The best-fitting parameters are $\Gamma = 2.46_{-0.23}^{+0.28}$, and $N_{\text{H}} < 7 \times 10^{20} \text{ cm}^{-2}$, with $C=520.8$ for 436 degrees of freedom. We note that the simple absorbed power law model does not provide a good representation of the data, leaving the significant residuals at the low energy of the spectra. X-ray studies of Seyfert 2 galaxies have shown that their spectra often show a soft excess at lower energy band, presumably due to a thermal emission component (e.g., Cappi et al. 2006). Thus we added an optically-thin thermal emission component (using the APEC model in XSPEC) to the absorbed power law. A significantly improved fit ($\Delta C = 89$ for two extra parameters) is obtained with best-fitting temperature of the thermal component $kT = 0.31_{-0.03}^{+0.02} \text{ keV}$. We then obtained the photon index $\Gamma = 1.54_{-0.27}^{+0.26}$, while the column density is constrained to be less than $3 \times 10^{20} \text{ cm}^{-2}$. When we add a narrow Gaussian line, with energy fixed at 6.4 keV (the rest energy of the Fe K α line) to the above model, the change of ΔC is less than 1 for addition of one free parameter, suggesting that the line is not detected. We therefore obtained an upper limit on the equivalent width (EW) of the line of $\sim 680 \text{ eV}$. The best-fitting model gives the observed $L_{0.5-2 \text{ keV}} = 2.7 \times 10^{39} \text{ erg s}^{-1}$ and $L_{2-10 \text{ keV}} = 2.9 \times 10^{39} \text{ erg s}^{-1}$. In Table 2, we show the best-fitting parameters, together with the model flux and luminosity in the 2-10 keV band. ³ The spectra are shown in Figure 4 (upper panel), together with the best-fit model and the residuals from the best-fit model.

Spatial analysis (Section 3.1) has shown that the X-ray emission of NGC 7590 is dominated by both the ULX and an extended component from the host galaxy. To probe the true nuclear emission due to the AGN, we performed a spectral extraction centered at the optically defined nucleus using a circular region of $9''$ radius (50% encircled-energy radius). The derived spectra could be best-fitted by an absorbed power law with $N_{\text{H}} < 4 \times 10^{20} \text{ cm}^{-2}$ and $\Gamma = 1.66_{-0.41}^{+0.35}$, plus a thermal component $kT = 0.32_{-0.05}^{+0.10} \text{ keV}$. The resulting X-ray flux $F_{2-10 \text{ keV}} = 1.6 \times 10^{-14} \text{ erg cm}^{-2} \text{ s}^{-1}$ (after aperture correction), and the upper limit to Fe K α line EW rises to 2060 eV (see Table 2). Note that the derived flux could serve as an upper limit to the nuclear X-ray emission in NGC 7590.

NGC 7590 X-1: NGC 7590 X-1 is an extranuclear X-ray source, originally detected in the *ROSAT* All-Sky Survey (Colbert & Ptak 2002). *XMM-Newton* spectra are well

³We note that Bassani et al. (1999) obtained a 2–10 keV flux of $1.2 \times 10^{-12} \text{ erg cm}^{-2} \text{ s}^{-1}$ for NGC 7590 based on *ASCA* data. This is much larger than the sum of the *XMM-Newton* flux of NGC 7590 and X-1, which is only $\sim 1.4 \times 10^{-13} \text{ erg cm}^{-2} \text{ s}^{-1}$. Through independent spectral fitting to archival *ASCA* data, we obtained an *ASCA* flux of $\sim 1.8 \times 10^{-13} \text{ erg cm}^{-2} \text{ s}^{-1}$, close to *XMM-Newton* results. The flux presented by Bassani et al. for NGC 7590 is thus incorrect and could be a typo.

fitted with an absorbed power-law model with $N_{\text{H}} = 5 \pm 2 \times 10^{21} \text{ cm}^{-2}$, $\Gamma = 2.13_{-0.12}^{+0.13}$, and $C/\text{dof}=657/758$. The observed 0.5–2 keV and 2–10 keV fluxes (after aperture correction) were $5.1 \times 10^{-14} \text{ erg cm}^{-2} \text{ s}^{-1}$ and $9.3 \times 10^{-14} \text{ erg cm}^{-2} \text{ s}^{-1}$, respectively. If the source is associated with NGC 7590, the implied 2–10 keV luminosity is $5.7 \times 10^{39} \text{ erg s}^{-1}$, making it as a ULX. The addition of a multicolor disk blackbody component is not statistically significant (C decreased by only 2.6 for the addition of two free parameters). The *XMM-Newton* spectra together with the best-fit model and residual are shown in Figure 4 (lower panel).

4. Discussion and Conclusions

NGC 7590 was previously identified as an "unobscured" Seyfert 2 galaxy, on the basis of the *ASCA* spectrum (Bassani et al. 1999). However, the poor X-ray spatial resolution of *ASCA* ($\sim 1'$ PSF FWHM) casts doubt that the X-ray flux may be contaminated by nearby bright sources. Thanks to its better spatial resolution ($\sim 6''$ PSF FWHM), the *XMM-Newton* data clearly show that the X-ray emission from NGC 7590 is dominated by an off-nuclear ULX and an extended component from the host galaxy.

By performing a spectral extraction using a circular region of $9''$ radius (50% encircled-energy radius), we gave an upper limit to the nuclei X-ray emission $F_{2-10 \text{ keV}} = 1.6 \times 10^{-14} \text{ erg cm}^{-2} \text{ s}^{-1}$ (after aperture correction). Although the best fitting N_{H} is less than $4 \times 10^{20} \text{ cm}^{-2}$, we find an upper limit to the T ratio ($f_{2-10 \text{ keV}}/f_{\text{O[III]}} < 0.09$)⁴. This value is in the range for the Compton-thick AGNs (Bassani et al. 1999; Guainazzi et al 2005). The Fe K α line was not detected with *XMM-Newton* and we could only obtain an upper limit of $\text{EW} < 2 \text{ keV}$, which is consistent with $\sim 1 \text{ keV}$ expected in the case of a Compton-thick AGN.

With *ASCA* data, Nicastro, Martocchia & Matt (2003) estimated that the accretion rate for NGC 7590 is very low ($< 10^{-4}$), suggesting it may intrinsically lack a BLR. Meanwhile, NGC 7590 has not shown a hidden BLR in polarized light (Heisler et al. 1997). Tran (2001) finds that the Seyfert 2 galaxies without hidden BLRs are those with the lowest luminosity, while Shu et al. (2007) suggested that the non-detection of hidden BLRs is ascribed to the large obscuration. Making use of L_{X} measured by *XMM-Newton*, we attempted to derive the accretion rate for NGC 7590 to determine whether it is still consistent with the Nicastro et al. (2003) results. If NGC 7590 is explained as Compton thick, the direct measurement of its intrinsic X-ray luminosity seems to be impossible. Thus, with a correction factor of 60 to its intrinsic luminosity (e.g., Panessa et al. 2006) and a black hole mass of $6.2 \times 10^6 M_{\odot}$

⁴ $f_{\text{O[III]}}$ has been extinction-corrected (Panessa & Bassani 2002).

derived from $M_{\text{BH}} - \sigma_*$ relation (Bian & Gu 2007), we obtain a rough estimate for NGC 7590 the accretion rate $\sim 2 \times 10^{-3}$, a value close to the threshold ($\sim 10^{-3}$) for BLR formation proposed by Nicastro et al. (2003). Note that Bian & Gu (2007) suggested the Nicastro et al. Eddington ratio threshold corresponds to an $L_{\text{bol}}/L_{\text{Edd}} \sim 10^{-1.37}$, if using [O III] λ 5007 (rather than X-ray) luminosity to estimate the bolometric luminosity. The $L_{\text{bol}}/L_{\text{Edd}}$ of $10^{-1.4}$ found for NGC 7590 using [O III] luminosity is more in agreement with the Nicastro et al. (2003) predictions, suggesting that NGC 7590 is likely genuinely lack of a BLR. However, XMM images suggest a Compton-thick obscuration to the nucleus of NGC 7590, thus supports the scenario that the non-detection of hidden BLR in this source could be attributed to heavy obscuration (see Shu et al. 2007), and the intrinsic lack of BLR is not necessarily required.

The *XMM-Newton* spectral fitting of NGC 7590 requires an additional soft component, which was well modeled with an emission spectrum from collisionally-ionized diffuse gas (the APEC model in XSPEC). The best-fit temperature for the soft thermal component is ~ 0.3 keV. This value is consistent with $KT \sim 0.2\text{--}0.8$ keV found in nearby Seyfert galaxies (Cappi et al. 2006), but lower than the range of gas temperatures (0.6–0.8 keV) found in LINERs (González-Martin et al. 2006). The inferred soft X-ray luminosity is $L_{0.5\text{--}2 \text{ keV}} \sim 2.7 \times 10^{39} \text{ erg s}^{-1}$. If the soft X-ray emission is originated from gas heated by intense star formation activities, the implied star formation rate for NGC 7590 is $\sim 1M_{\odot} \text{ yr}^{-1}$ (Rovilos et al. 2009), which is consistent with the estimate using its far-infrared luminosity (Kennicutt 1998).

In summary, *XMM-Newton* observations reveal that the X-ray emission of NGC 7590 is dominated by an extended component and an off-nuclear ULX. This indicates that its pre-identified "unobscured" nature is likely artificial. Due to the contamination from the ULX and the extended component, we are unable to isolate the nuclear X-ray emission for NGC 7590, and the flux upper limit was given. The derived relatively small T ratio suggests that the galaxy likely has a heavily obscured nucleus, which could be confirmed with higher spatial resolution *Chandra* images. Future hard X-ray imaging telescopes (i.e., NUSTAR, ASTRO-H) could also help by detecting the hard X-ray bump at $\sim 20 - 30$ keV of the Compton-thick spectrum.

This research made use of the HEASARC online data archive services, supported by NASA/GSFC. The work was supported by Chinese NSF through Grant 10773010/10825312, and the Knowledge Innovation Program of CAS (Grant No. KJCX2-YW-T05).

REFERENCES

Antonucci, R. 1993, ARA&A, 31, 473

- Barcons X., Carrera F. J., Ceballos M. T., 2003, MNRAS, 339, 757
- Bassani, L., Dadina, M., Maiolino, et al. 1999, ApJS, 121, 473
- Bian, W., & Gu, Q. 2007, ApJ, 657, 159
- Bianchi S., Corral A., & Panessa F., et al. 2008, MNRAS, 385, 195
- Brightman M., Nandra K., 2008, MNRAS, 390, 1241
- Caccianiga A. et al., 2004, A&A, 416, 901
- Cappi M. et al., 2006, A&A, 446, 459
- Cash, W. 1979, ApJ, 228, 939
- Colbert, E. J. M., & Ptak, A. F. 2002, ApJS, 143, 25
- Corral A., Barcons X., Carrera F. J., Ceballos M. T., Mateos S., 2005, A&A, 431, 97
- Dickey, J. M., & Lockman, F. J. 1990, ARA&A, 28, 215
- Georgantopoulos, I., & Zesas, A. 2003, ApJ, 594, 704
- Ghosh, H., et al. 2007, ApJ, 656, 105
- Glozzi M., Sambruna R. M., Foschini L., 2007, ApJ, 662, 878
- Guainazzi, M., Matt, G., & Perola, G. C. 2005, A&A, 444, 119
- González-Martin, O., Masegosa, J., Márquez, I. et al. 2006, A&A, 460, 45
- Heisler, C. A., Lumsden, S. L., & Bailey, J. A. 1997, Nature, 385, 700
- Kennicutt, R. C., Jr. 1998, ApJ, 498, 541
- Markowitz, A., & Edelson, R. 2004, ApJ, 617, 939
- Moran, E. C., Barth, A. J., Kay, L. E., & Filippenko, A. V. 2000, ApJ, 540, L73
- Nicastro, F. 2000, ApJ, 530, L65
- Nicastro, F., Martocchia, A., & Matt, G. 2003, ApJ, 589, L13
- Panessa, F., & Bassani, L. 2002, A&A, 394, 435
- Panessa, F., Bassani, L., Cappi, M. et al. 2006, A&A, 455, 173

- Panessa, F., Carrera, F. J., Bianchi, S., et al. 2009, MNRAS, 398, 1951
- Pappa, A., Georgantopoulos, I., Stewart, G. C., & Zezas, A. L. 2001, MNRAS, 326, 995
- Risaliti G., Maiolino R., Salvati M., 1999, ApJ, 522, 157
- Rovilos, E., Georgantopoulos, I., Tzanavaris, P. et al. 2009, A&A, 502, 85
- Rush B., Malkan M. A., Spinoglio L., 1993, ApJS, 89, 1
- Shi, Y., Rieke, G. H., Smith, P., Rigby, J., Hines, D., Donley, J., Schmidt, G., & Diamond-Stanic, A. M. 2010, ApJ, 714, 115
- Shu, X. W., Wang, J. X., Jiang, P., Fan, L. L., & Wang, T. G. 2007, ApJ, 657, 167
- Tran, H. D. 2001, ApJ, 554, L19
- Wolter, A., Gioia, I. M., Henry, J. P., & Mullis, C. R. 2005, A&A, 444, 165

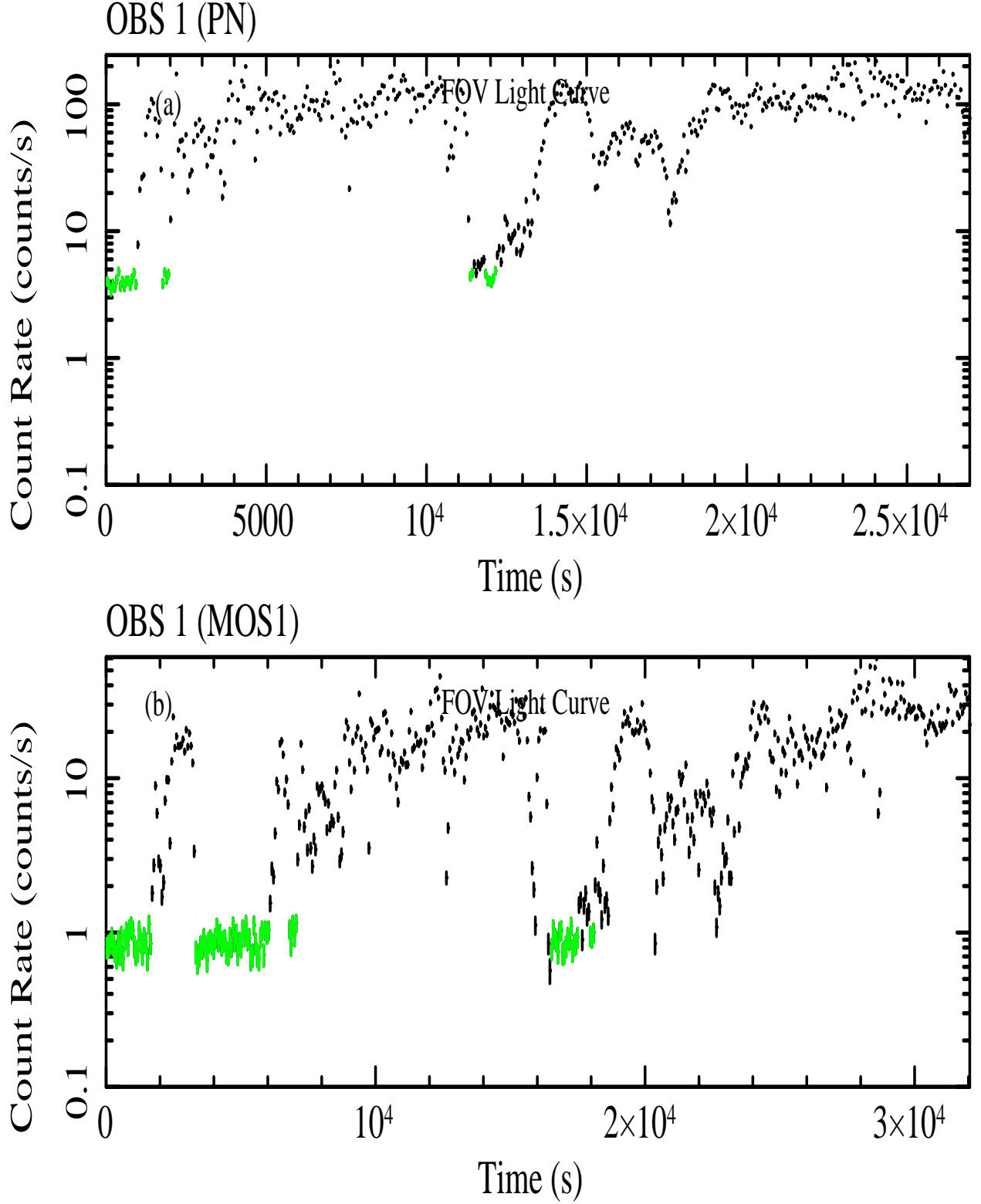


Fig. 1.— FOV light curves for OBS1 (black) and filtered good time intervals (green) by *espfilt*.

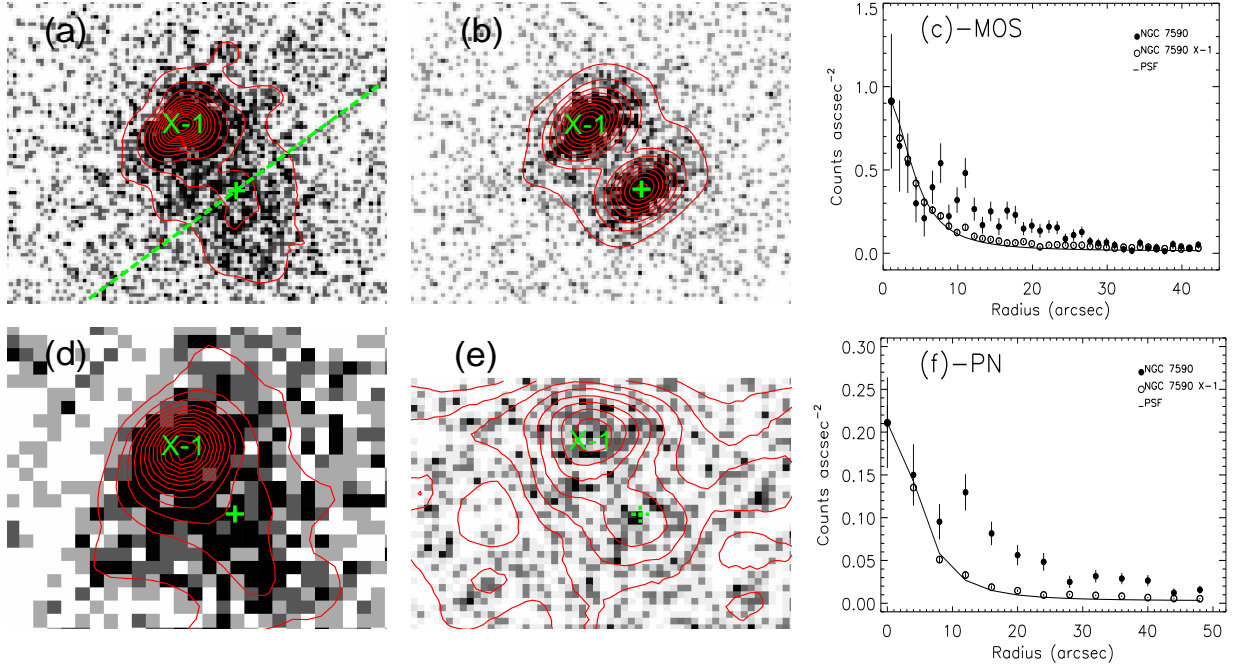


Fig. 2.— *Left:* *XMM-Newton* MOS (upper) and pn (lower) images of NGC 7590 with X-ray contours overlaid. The cross denotes the optical nucleus of the galaxy. Source X-1 denotes the off-nuclear ULX. *Middle:* Simulated EPIC MOS image of two point sources (upper). The lower panel is ROSAT HRI image. *Right:* The observed MOS and pn radial profiles of the NGC 7590 (filled circles), ULX (open circles), compared with the *XMM-Newton* PSF (solid lines). The data points are normalized to the peak brightness of NGC 7590. While extracting radial profiles for NGC 7590, only photons below the dashed line in panel (a) were included to avoid contaminations from the ULX.

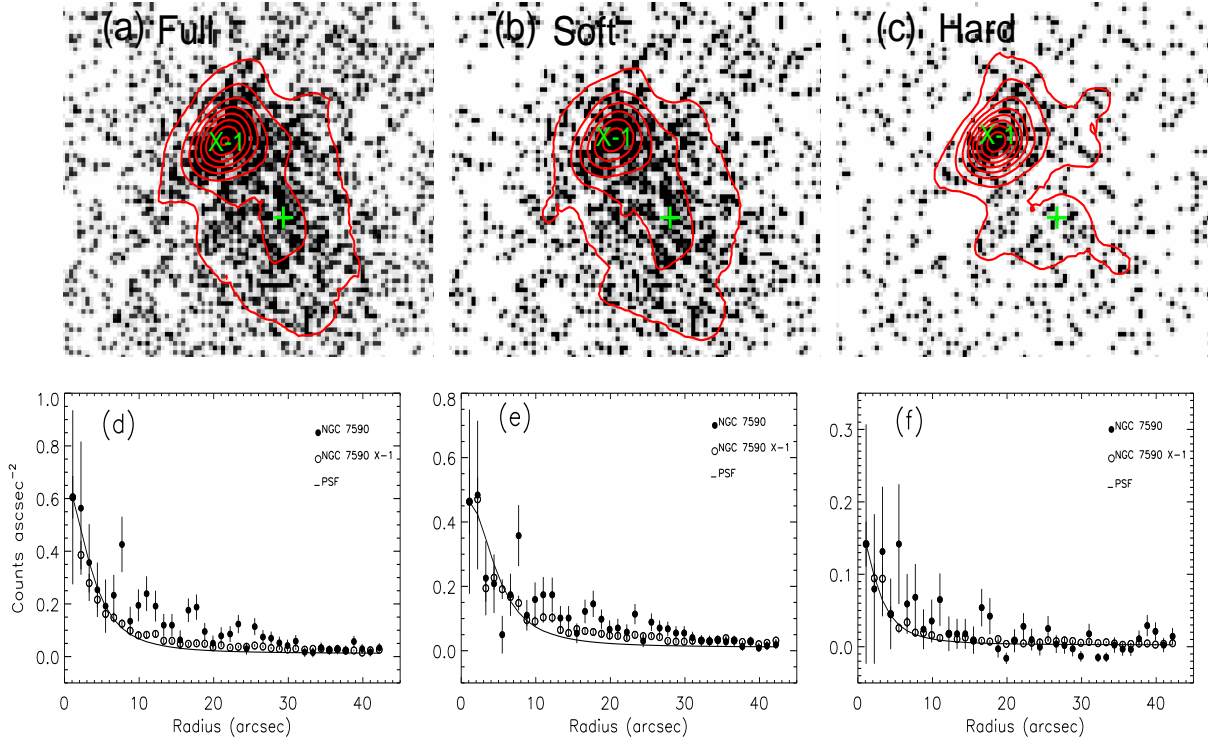


Fig. 3.— Co-added MOS images for OBS 3 at different bands with X-ray contours overlaid (upper), and associated radial profile of ULX and NGC 7590, compared to the XMM PSF model (lower). The cross denotes the optical nucleus of the galaxy. Source X-1 denotes the off-nuclear ULX. *Left*: 0.3-10 keV; *Middle*: 0.3-2 keV; *Right*: 2-10 keV.

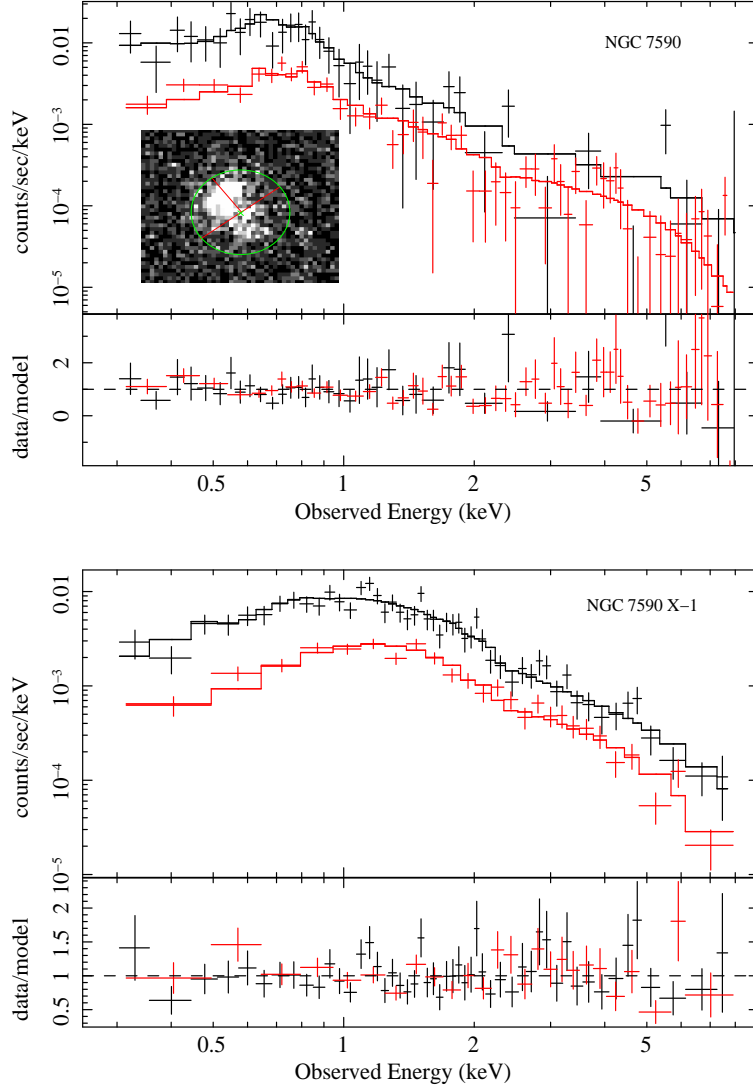


Fig. 4.— EPIC pn (black) and MOS (red) spectra of NGC 7590 (upper) and ULX (lower), together with the best-fitting model and the ratio of the data to the model. The inset is the co-added pn and MOS image for OBS 2 to demonstrate how the source spectra were extracted for NGC 7590 (see the text for details).

Table 1. *XMM-Newton* Observations of NGC 7590

ObsID	Rev.	Date	Net. Exp. (ks) (pn/MOS1/MOS2)
0405380701 (OBS 1)	1353	2007 Apr 30	1.5/5.8/5.8
0112310201 (OBS 2)	0267	2001 May 25	13.4/20.2/21.1
0204610101 (OBS 3)	0987	2005 Apr 29	52.2/64.5/65.1

Table 2. Results of X-ray spectral fitting

Target (1)	N_{H} (2)	Γ (3)	KT (4)	$\text{EW}_{6.4}$ (5)	$F_{2-10 \text{ keV}}$ (6)	$L_{2-10 \text{ keV}}$ (7)	C/dof (8)
ULX	0.25 ± 0.04	$2.13^{+0.13}_{-0.12}$	9.3	5.7	657/758
NGC 7590	< 0.03	$1.54^{+0.26}_{-0.27}$	$0.31^{+0.02}_{-0.03}$	< 680	4.8	2.9	431/433
NGC 7590 (nucleus)	< 0.04	$1.66^{+0.35}_{-0.41}$	$0.32^{+0.10}_{-0.05}$	< 2060	1.6	1.0	185/168

Note. — Col.(1): target. Col.(2): column density of absorbed power-law in units of 10^{22} cm^{-2} . Col.(3) photon index. Col.(4): temperature of the thermal component in keV. Col.(5): EW of Fe $K\alpha$ line in eV. Col.(6): model flux in the 2–10 keV band, in units of $10^{-14} \text{ erg cm}^{-2} \text{ s}^{-1}$ (after aperture correction). Col. (7): observed luminosity in the 2–10 keV band, in units of $10^{39} \text{ erg s}^{-1}$. Col. (8): C and degrees of freedom.